The Free Boundary SABR: Natural Extension to Negative Rates

Alexandre Antonov, Michael Konikov and Michael Spector
Numerix

January 28, 2015

Abstract

In the current low-interest-rate environment, extending option models to negative rates has become an important issue. This paper[1] describes one such extension of the widely used SABR model. *We stress that our solution is more natural and attractive than the shifted SABR.* An exact formula is derived for the option prices in the case of zero correlation between the rate and its volatility. For nonzero correlation, a mapping procedure onto a mimicking zero-correlation model is applied. Analytical results for the suggested free-boundary SABR model are compared with Monte Carlo simulations.

1 Introduction

The classical SABR process [7] for a rate F_t and stochastic volatility v_t has the SDE

$$dF_t = F_t^{\beta}\, v_t\, dW_1,$$
$$dv_t = \gamma\, v_t\, dW_2,$$

with some correlation $E[dW_2\, dW_1] = \rho dt$ and power $0 \le \beta < 1$. The solution is not uniquely define by the SDE—we also need to impose some boundary conditions. The standard choice is to use an absorbing boundary at zero and enforce the positivity and martingality of the rate. See [1], [3], [5], [8], [9], [10], [12] for further references.

The SABR model is primarily used for volatility cube interpolation and for pricing CMS products by replication with vanilla option prices. It is also used in term structure models, e.g., [11], [13].

In current market conditions, when rates are extremely low and sometimes even negative, it is important to extend the SABR model to negative rates. The simplest way is to model the shifted rate

$$F'_t = F_t + s_t$$

as a SABR process, where s_t is a deterministic positive shift. An obvious drawback of this approach is the a priori selection of the shift, since we do not know in advance how low the rates can go, and we may end up in a situation when we need to change the value of this shift and recompute PV and risk of our entire portfolio. We need a more natural solution to permit negative rates.

[1] It was first presented at the 10th Fixed Income Conference, WBS (October 2014, Barcelona)

Electronic copy available at: http://ssrn.com/abstract=2557046

For $\beta = 0$, the normal SABR model

$$dF_t = v_t\, dW_1$$

allows the rates to become negative when a free boundary condition is enforced. Below we come up with a general "extrapolated" model

$$dF_t = |F_t|^\beta\, v_t\, dW_1$$

with $0 \le \beta < \frac{1}{2}$, and a *free* boundary.

In what follows, we consider only the $F_0 > 0$ case. When $F_0 < 0$, we note that $\tilde{F}_t = -F_t$ satisfies the SDE

$$\begin{aligned} d\tilde{F}_t &= -dF_t = -|\tilde{F}_t|^\beta\, v_t\, dW_1 = |\tilde{F}_t|^\beta\, v_t\, d\tilde{W}_1, \\ dv_t &= \gamma\, v_t\, dW_2, \end{aligned}$$

where $\tilde{W}_1 = -W_1$, which implies that $\tilde{F}_t$ is a free-boundary SABR process with parameters $(-F_0, \alpha, \beta, -\rho, \gamma)$. For the time value of a European option, we have

$$\begin{aligned} \mathcal{O}^F(T,K) &= \mathbb{E}\left[(F_T - K)^+\right] - (F_0 - K)^+ = \mathbb{E}\left[(-K - (-F_T))^+\right] - (-K - (-F_0))^+ \\ &= \mathbb{E}\left[\left(\tilde{K} - \tilde{F}_T\right)^+\right] - \left(\tilde{K} - \tilde{F}_0\right)^+ = \mathcal{O}^{\tilde{F}}(T,\tilde{K}), \end{aligned}$$

where $\tilde{K} = -K$.

To get intuition about the free boundary, we start with CEV example $dF_t = |F_t|^\beta\, dW$ and study the PDF and the option prices. Then we switch to a SABR model with negative values and a free boundary condition and derive an exact solution for the zero-correlation case. For the general case, we show an accurate approximation for pricing European options. We finish with simulation schemes and numerical results.

2 CEV process

2.1 Absorbing and Reflecting solutions

To aid with intuition, we consider the CEV model

$$dF_t = F_t^\beta\, dW \tag{1}$$

with $0 \le \beta < 1$. Consider the forward Kolmogorov (FK) equation on the density $p(t,f)$

$$p_t - \frac{1}{2}\left(f^{2\beta}\, p\right)_{ff} = 0. \tag{2}$$

The flow $j(t,f)$ is defined by the continuity equation

$$p_t + j_f = 0 \;\;\rightarrow\;\; j(t,f) = -\frac{1}{2}\left(f^{2\beta}\, p\right)_f. \tag{3}$$

Electronic copy available at: http://ssrn.com/abstract=2557046

The FK equation has two types solutions depending on the boundary conditions, so fixing the PDE (or SDE) alone is not sufficient to uniquely define the solution.

Let us briefly describe the procedure. To calculate the asymptotics at small f, one should introduce the ansatz

$$p(t,f) = f^{\kappa}\, F(t,x)$$

in the FK equation, where $F(t,x)$ is a regular function of $x = f^{2(1-\beta)}$ and the index κ is determined by zeroing the coefficient in the term with the lowest power of f. This gives distinct solutions with asymptotics $p_A \sim f^{1-2\beta}$ and $p_R \sim f^{-2\beta}$. We call the first solution "absorbing" and the second one "reflecting". The latter exists only for $\beta < \frac{1}{2}$; otherwise, the norm around zero diverges.

The asymptotics are closely related to conservation laws, which can be obtained by integrating the FK equation by parts with some payoff $h(f)$; i.e.,

$$\begin{aligned}\partial_t \left(\int_0^\infty df\, h(f)\, p(t,f) \right) &= \frac{1}{2} \int_0^\infty df\, h(f)\, \left(f^{2\beta}\, p(t,f) \right)_{ff} \\ &= \frac{1}{2} \int_0^\infty df\, h''(f)\, f^{2\beta}\, p(t,f) + \frac{1}{2} \left[h'(f)\, f^{2\beta}\, p(t,f) - h(f) \left(f^{2\beta}\, p(t,f) \right)_f \right]_{f=0}.\end{aligned} \tag{4}$$

Consider first the norm case of $h(f) = 1$. It is easy to see the asymptotics of the absorbing solution leads to nonconservation of the norm, while the reflecting solution conserves the norm. For the first moment conservation, we take $h(f) = f$ and deduce that the asymptotics of the reflecting solution leads to nonconservation of the first moment (i.e., nonmartingality), while the absorbing solution is a martingale.

The main properties of the absorbing and reflecting solutions are summarized in Table 1.

Type	**Absorbing**	**Reflecting**
PDF asymptotics	$p_A \sim f^{1-2\beta}$	$p_R \sim f^{-2\beta}$
Flow asymptotics		
$j(t,f) = -\frac{1}{2} \left(f^{2\beta}\, p \right)_f$	$j_1 = const$	$j_2 = 0$
Norm conservation		
$\partial_t n(t) = j(t,0)$	no	yes
First moment conservation		
$\partial_t m(t) = -\frac{1}{2} \left[f \left(f^{2\beta}\, p \right)_f - f^{2\beta}\, p \right]_{f=0}$	yes	no

Table 1: Summary of properties of absorbing and reflecting solutions.

The explicit PDFs for the CEV process are known (see [6]) and given by

$$p_A(t,f) = \frac{1}{1-\beta}\frac{f^{1-2\,\beta}}{t}\,\left(\frac{f}{f_0}\right)^{-\frac{1}{2}}\,e^{-\frac{q^2+q_0^2}{2\,t}}I_{|\nu|}\left(\frac{q\,q_0}{t}\right),$$
$$p_R(t,f) = \frac{1}{1-\beta}\frac{f^{1-2\,\beta}}{t}\,\left(\frac{f}{f_0}\right)^{-\frac{1}{2}}\,e^{-\frac{q^2+q_0^2}{2\,t}}I_{\nu}\left(\frac{q\,q_0}{t}\right),$$

for

$$\nu = -\frac{1}{2(1-\beta)}$$

with

$$q_0 = \frac{f_0^{1-\beta}}{1-\beta} \quad \text{and} \quad q = \frac{f^{1-\beta}}{1-\beta}.$$

Here $I_\nu(x)$ is the modified Bessel function of order ν.

The call option payoff for $K > 0$

$$h(f) = (f-K)^+$$

results in the usual formula without boundary terms

$$\partial_t\left(\int_0^\infty df\,(f-K)^+\,p(t,f)\right) = \frac{1}{2}K^{2\beta}\,p(t,K) \tag{5}$$

for both reflecting and absorbing solutions. The option time-value $\mathcal{O}(T,K)$ becomes

$$\mathcal{O}(T,K) = \mathbb{E}[(F_T-K)^+] - (F_0-K)^+ = \frac{1}{2}K^{2\beta}\int_0^T dt\,p(t,K). \tag{6}$$

Note that it is not the case for put options, where a boundary term is present.

Below we will need option prices for absorbing/reflecting solutions via a 1D integral:

$$\mathcal{O}_{A/R}(T,K) = \frac{\sqrt{K\,F_0}}{\pi}\left(\int_0^\pi \frac{\sin(|\nu|\,\theta)\sin(\theta)}{b-\cos(\theta)}e^{-\frac{\bar{q}(b-\cos(\theta))}{T}}d\theta\right.$$
$$\left. + \sin(|\nu|\,\pi)\int_0^\infty \frac{e^{\mp|\nu|x}\sinh(x)}{b+\cosh(x)}e^{-\frac{\bar{q}(b+\cosh(x))}{T}}dx\right) \tag{7}$$

for

$$\bar{q} = q_0\,q_K \quad \text{with} \quad b = \frac{q_0^2+q_K^2}{2\,q_0\,q_K}.$$

This formula was derived in [4] for the absorbing case.

2.2 CEV with the free boundary condition

Now we consider an extension of the CEV model to the entire real line F by modifying the SDE to

$$dF_t = |F_t|^\beta\,dW \tag{8}$$

for $0 \leq \beta < \frac{1}{2}$. The corresponding forward Kolmogorov (FK) equation is

$$\partial_t\, p(t,f) = \frac{1}{2}\left(|f|^{2\beta}\, p(t,f)\right)_{ff}. \tag{9}$$

For positive and negative values, we have

$$\begin{aligned}
\partial_t\, p(t,f) &= \frac{1}{2}\left(f^{2\beta}\, p(t,f)\right)_{ff} \quad \text{for} \quad f>0,\\
\partial_t\, p(t,f) &= \frac{1}{2}\left((-f)^{2\beta}\, p(t,f)\right)_{ff} \quad \text{for} \quad f<0.
\end{aligned}$$

The flow $j(t,f)$ is defined by the continuity equation $p_t + j_f = 0$ and is equal to

$$j(t,f) = -\frac{1}{2}\left(|f|^{2\beta}\, p\right)_f. \tag{10}$$

A solution that satisfies the FK equation with the initial condition $p(0,f) = \delta(f-f_0)$ can be constructed from the reflecting and absorbing solutions as

$$p(t,f) = \frac{1}{2}\left(p_R(t,|f|) + \text{sign}(f)\; p_A(t,|f|)\right), \tag{11}$$

or

$$\begin{aligned}
p(t,f) &= \frac{1}{2}\left(p_R(t,f) + p_A(t,f)\right) \quad \text{for} \quad f>0,\\
p(t,f) &= \frac{1}{2}\left(p_R(t,-f) - p_A(t,-f)\right) \quad \text{for} \quad f<0,
\end{aligned}$$

which guarantees the desired initial condition and continuity of the flow.

The solutions for typical parameters are shown in Figure 1. The blue solid line represents the free PDF, the red dotted line depicts the absorbing density expression $\text{sign}(f)\; p_A(t,|f|)$ while the green dashed line gives the symmetrized reflecting solution.

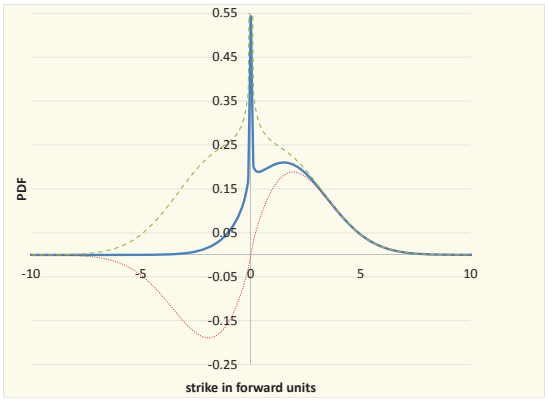

Figure 1: Free PDF (blue solid), absorbing density (red dotted), and symmetrized symmetric (green dashed) solutions to the FK equation for typical parameter values.

We can get the same expression for density with a purely probabilistic argument. For any $f > 0$, a reflecting path ending at f is equivalent to a free-boundary path ending at f or $-f$, and vice versa. For the absorbing case, we apply the reflection principal as usual, which is to take the probability of path ending at f and subtract the probability of path ending at f and touching zero, which is equivalent to a path ending at $-f$. Hence, we can write the linear system

$$p_R(t, f) = p(t, f) + p(t, -f),$$
$$p_A(t, f) = p(t, f) - p(t, -f),$$

which yields the expression for the free boundary density upon solving.

We see that the SDE does not determine the process—we need extra information on the boundary. The intuition behind our free CEV works as follows. Instead of sticking at zero (the "absorbing" condition), the "free" particle flows across the zero boundary to the negative axis.

Note that at zero the PDF diverges as $p(t, f) \sim |f|^{-2\,\beta}$. The probability of the rate being in an ϵ-vicinity around zero is $\sim \epsilon^{1-2\,\beta}$. One can regularize this singularity by using $dF_t = (F_t^2 + \epsilon^2)^{\frac{\beta}{2}}\, dW$ for small ϵ. However, this will hardly lead to an analytical solution.

For visualization, Figures 2 and 3 show graphs of the free CEV PDF (11) with the parameters in Table 2. These settings correspond to the typical ATM normal implied volatility of $\sigma_N \simeq F_0^{\beta}\, v_0 = 30\, bps$ or the equivalent lognormal volatility $\sigma_{LN} \simeq F_0^{\beta-1}\, v_0 = 60\%$.

Parameter	Symbol	Value
Rate Initial Value	F_0	50 bps
SV Initial Value	v_0	$0.6\, F_0^{1-\beta}$
Skews	β	0.1 and 0.25
Maturities	T	3Y

Table 2: Setups for the CEV model for the plots in Figures 2 and 3.

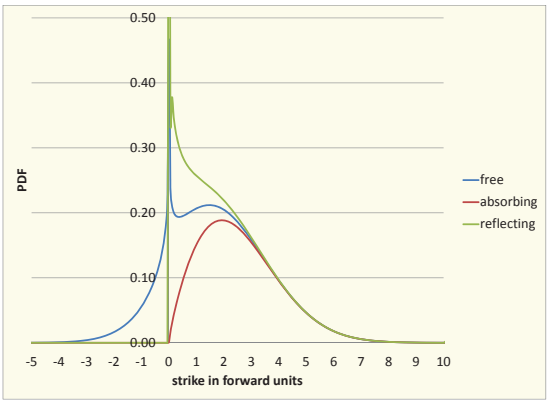

Figure 2: PDF with different boundary conditions for $T = 3Y$, $\beta = 0.1$.

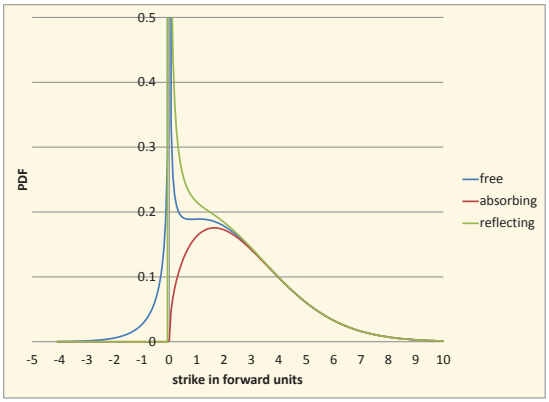

Figure 3: PDF with different boundary conditions for $T = 3Y$, $\beta = 0.25$.

The observed singularity is modest (especially for typical β and short maturities, where the negative rates are observed) with respect to the δ-functional singularity for the classical absorbing case. As we will see below, the SABR spikes are less pronounced than the CEV ones.

To study conservation laws of the free CEV, we integrate the free FK with a payoff $h(f)$ over the entire axis:

$$\partial_t \left(\int_{-\infty}^{+\infty} df\, h(f)\, p(t,f) \right) = \frac{1}{2} \int_{-\infty}^{+\infty} df\, h''(f)\, |f|^{2\beta}\, p(t,f) + \frac{1}{2} \left[h'(f)\, |f|^{2\beta}\, p(t,f) - h(f) \left(|f|^{2\beta}\, p(t,f) \right)_f \right]_{-0}^{+0}.$$

The asymptotic behavior at zero is inherited from the reflecting solution $p(t,f) \sim |f|^{-2\beta}$. One can check the conservation of both norm and the first moment in the free CEV.

A call option payoff $h(f) = (f-K)^+$ leads to an option time-value of

$$\begin{aligned} \mathcal{O}_F(T,K) &= \frac{1}{2}|K|^{2\beta} \int_0^T dt\, p(t,K) \\ &= \frac{1}{2}|K|^{2\beta} \int_0^T dt\, \frac{1}{2} \left(p_R(t,|K|) + \mathrm{sign}(K)\; p_A(t,|K|) \right) \\ &= \frac{1}{2} \left(\mathcal{O}_R(T,|K|) + \mathrm{sign}(K)\, \mathcal{O}_A(T,|K|) \right). \end{aligned} \tag{12}$$

Clearly, the call option price $\mathcal{O}_F(T,K)$ is smooth for $K=0$. The normal implied vol from $\mathcal{O}_F(T,K)$ is plotted in Figure 4, and we can see that there is no weird behavior around zero.

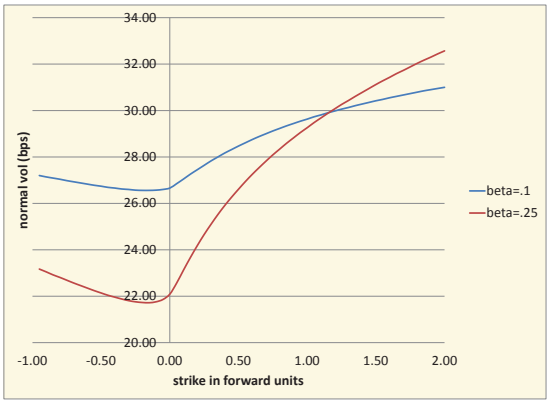

Figure 4: Normal implied vol for a $T = 3Y$ call.

Finally, we present the free CEV option integral. Its time-value can be easily derived from the absorbing-reflecting solutions (7) and (12), yielding

$$\begin{aligned} \mathcal{O}_F(\tau,K) = \frac{\sqrt{|K|F_0}}{\pi} \Bigg(& \mathbf{1}_{K\geq 0} \int_0^\pi \frac{\sin(\eta\theta)\sin\theta}{b-\cos\theta}\, e^{-\frac{\bar{q}(b-\cos\theta)}{\tau}}\, d\theta \\ & + \sin(\eta\pi) \int_0^\infty \frac{(\mathbf{1}_{K\geq 0}\cosh\eta x + \mathbf{1}_{K<0}\sinh\eta x)\sinh x}{b+\cosh x}\, e^{-\frac{\bar{q}(b+\cosh x)}{\tau}}\, dx \Bigg), \end{aligned} \tag{13}$$

where $\eta = |\nu|$ and

$$\bar{q} = \frac{|f_0\, f|^{1-\beta}}{(1-\beta)^2} \quad \text{with} \quad b = \frac{|f_0|^{2(1-\beta)} + |f|^{2(1-\beta)}}{2\,|f_0\, f|^{1-\beta}}.$$

We will use this formula to derive analytics for the SABR model in the section below.

3 SABR

Now, let us come back to the SABR process

$$\begin{aligned} dF_t &= F_t^{\beta}\, v_t\, dW_1, \\ dv_t &= \gamma\, v_t\, dW_2. \end{aligned}$$

The standard choice of the absorbing boundary will be generalized to the *free* boundary. Namely, we will consider the SDE

$$dF_t = |F_t|^{\beta}\, v_t\, dW_1$$

for $0 \le \beta < \frac{1}{2}$, which permits the *negative* rates.

Looking forward, we use our results to graph the SABR density function, which is shown in Figures 5 and 6 for the parameters in Table 3. We will see that the singularity at zero is almost negligible.

Parameter	**Symbol**	**Value**
Rate Initial Value	F_0	50 bps
SV Initial Value	v_0	$0.6\, F_0^{1-\beta}$
Vol-of-Vol	γ	0.3
Correlations	ρ	-0.3
Skews	β	0.1 and 0.25
Maturities	T	3Y

Table 3: Setups for the SABR model for the plots in Figures 5 and 6.

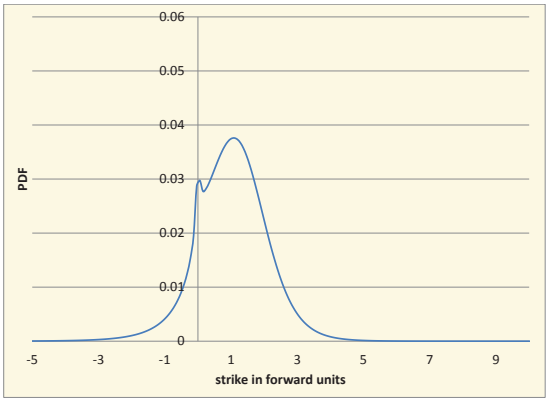

Figure 5: SABR model PDF for $T = 3Y$, $\beta = 0.1$.

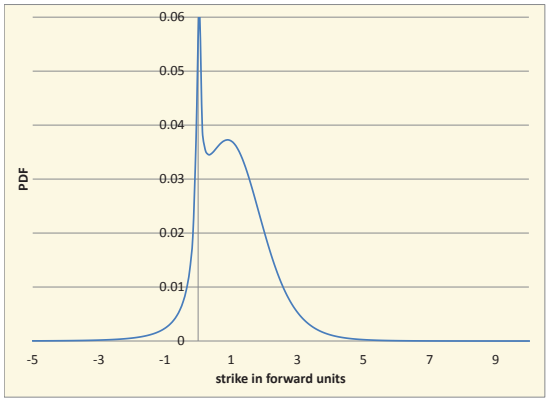

Figure 6: SABR model PDF for $T = 3Y$, $\beta = 0.25$.

3.1 Zero-correlation case

The zero-correlation free SABR model can be solved exactly. Indeed, the option price can be computed as

$$\mathcal{O}_F^{SABR}(T,K) = E\left[\mathcal{O}_F^{CEV}(\tau_T,K)\right], \tag{14}$$

where $\mathcal{O}_F^{CEV}(\tau,K)$ is the free-boundary CEV option price (13) and the stochastic time

$$\tau_T = \int_0^T v_t^2 dt \tag{15}$$

is the cumulative variance for the geometric Brownian motion v_t. The dependence on τ in both integrand terms of (13) is of the form $\exp\left(-\frac{\lambda}{\tau}\right)$. Thus, averaging over stochastic time,

$$E\left[\mathcal{O}_F^{CEV}(\tau_T,K)\right],$$

requires calculating the mean value

$$E\left[\exp\left(-\frac{\lambda}{\tau}\right)\right].$$

The moment generating function (MGF) of the inverse stochastic time was derived in [4]

$$E\left[\exp\left(-\frac{\lambda}{\tau}\right)\right] = \frac{G(T\,\gamma^2, s)}{\cosh s}\,, \tag{16}$$

$$G(t,s) = 2\sqrt{2}\frac{e^{-\frac{t}{8}}}{t\sqrt{2\pi t}}\int_s^\infty du\, u\, e^{-\frac{u^2}{2t}}\sqrt{\cosh u - \cosh s}\,, \tag{17}$$

$$s = \sinh^{-1}\left(\frac{\sqrt{2\lambda}\,\gamma}{v_0}\right). \tag{18}$$

The function $G(t,s)$ has been introduced in [3]: it is closely related to the McKean heat kernel on the hyperbolic plane H^2. It is important to notice that, although then function $G(t,s)$ is a 1D integral, it can be very efficiently approximated by a closed formula (see [3]).

Thus, the exact option price for the zero correlation case can be presented as

$$\mathcal{O}_F^{SABR}(T,K) = \frac{1}{\pi}\sqrt{KF_0}\,\{\mathbf{1}_{K\geq 0}A_1 + \sin(|\nu|\,\pi)\,A_2\}$$

with integrals

$$A_1 = \int_0^\pi d\phi \frac{\sin\phi \sin\left(|\nu|\,\phi\right)}{b-\cos\phi}\frac{G(T\,\gamma^2, s(\phi))}{\cosh s(\phi)}, \tag{19}$$

$$A_2 = \int_0^\infty d\psi \frac{\sinh\psi\,(\mathbf{1}_{K\geq 0}\cosh(|\nu|\,\psi) + \mathbf{1}_{K<0}\sinh(|\nu|\,\psi))}{b+\cosh\psi}\,\frac{G(T\,\gamma^2, s(\psi))}{\cosh s(\psi)}. \tag{20}$$

Here s has the following parameterization with respect to ϕ and ψ:

$$\sinh s(\phi) = \gamma\, v_0^{-1}\,\sqrt{2\bar{q}(b-\cos\phi)},$$
$$\sinh s(\psi) = \gamma\, v_0^{-1}\,\sqrt{2\bar{q}(b+\cosh\psi)},$$

where $\bar{q}$ and b are the same as in the CEV free-boundary option.

3.2 General correlation case

As in [3], we approximate the general correlation option price by using the zero correlation one

$$d\tilde{F}_t = |\tilde{F}|_t^{\tilde{\beta}}\,\tilde{v}_t\,d\tilde{W}_1,$$
$$d\tilde{v}_t = \tilde{\gamma}\,\tilde{v}_t\,d\tilde{W}_2,$$

with $\mathbb{E}[d\tilde{W}_1\,d\tilde{W}_2] = 0$, i.e.,

$$E\left[(F_t-K)^+\right] \simeq E\left[(\tilde{F}_t-K)^+\right].$$

For the *free* boundary, we reuse the same effective coefficients of the zero-correlation SABR as in AKS (2013) (*absorbing* boundary):

- Strike-independent parameters: the power and vol are simply

$$\tilde{\beta} = \beta, \tag{21}$$

$$\tilde{\gamma}^2 = \gamma^2 - \frac{3}{2}\left\{\gamma^2\rho^2 + v_0\gamma\rho\,(1-\beta)\,F_0^{\beta-1}\right\}. \tag{22}$$

- Strike-dependent parameters: the initial stochastic volatility value $\tilde{v}_0$ can be calculated as an expansion

$$\tilde{v}_0 = \tilde{v}_0^{(0)} + T\,\tilde{v}_0^{(1)} + \cdots. \tag{23}$$

The leading volatility term can be expressed as

$$\tilde{v}_0^{(0)} = \frac{2\,\Phi\,\delta\tilde{q}\,\tilde{\gamma}}{\Phi^2 - 1}, \tag{24}$$

where

$$\Phi = \left(\frac{v_{\min} + \rho v_0 + \gamma\,\delta q}{(1+\rho)v_0}\right)^{\frac{\tilde{\gamma}}{\gamma}} \quad \text{and} \quad v_{\min}^2 = \gamma^2\delta q^2 + 2\gamma\rho\delta q v_0 + v_0^2$$

for

$$\delta q = \frac{|k|^{1-\beta} - |F_0|^{1-\beta}}{1-\beta} \quad \text{and} \quad \delta\tilde{q} = \frac{|k|^{1-\tilde{\beta}} - |F_0|^{1-\tilde{\beta}}}{1-\tilde{\beta}}. \tag{25}$$

The effective strike k is a *floored* initial strike: all the effective parameters formulae based on the heat-kernel expansion work for positive strikes. In our experiments, we used

$$k = \max(K, 0.1\,F_0).$$

The first-order correction is more complicated and is given by

$$\frac{\tilde{v}_0^{(1)}}{\tilde{v}_0^{(0)}} = \tilde{\gamma}^2\,\sqrt{1+\tilde{R}^2}\,\frac{\frac{1}{2}\ln\left(\frac{v_0 v_{\min}}{\tilde{v}_0^{(0)}\tilde{v}_{\min}}\right) - \mathcal{B}_{\min}}{\tilde{R}\,\ln\left(\sqrt{1+\tilde{R}^2}+\tilde{R}\right)} \quad \text{for} \quad \tilde{R} = \frac{\delta q\,\tilde{\gamma}}{\tilde{v}_0^{(0)}},$$

where

$$\tilde{v}_{\min} = \sqrt{\tilde{\gamma}^2\delta q^2 + \left(\tilde{v}_0^{(0)}\right)^2}$$

and $\mathcal{B}_{\min}$ is the so-called parallel transport, defined as

$$\mathcal{B}_{\min} = -\tfrac{1}{2}\frac{\beta}{1-\beta}\frac{\rho}{\sqrt{1-\rho^2}}\,(\pi - \varphi_0 - \arccos\rho - I)\,. \tag{26}$$

Here we have

$$L = \frac{v_{\min}}{q\,\gamma\,\sqrt{1-\rho^2}} \quad \text{and} \quad \varphi_0 = \arccos\left(-\frac{\delta q\,\gamma + v_0\,\rho}{v_{\min}}\right)$$

and

$$I = \begin{cases} \frac{2}{\sqrt{1-L^2}}\left(\arctan\frac{u_0+L}{\sqrt{1-L^2}} - \arctan\frac{L}{\sqrt{1-L^2}}\right) & \text{for } L<1, \\ \frac{1}{\sqrt{L^2-1}}\ln\frac{u_0\left(L+\sqrt{L^2-1}\right)+1}{u_0\left(L-\sqrt{L^2-1}\right)+1} & \text{for } L>1, \end{cases} \tag{27}$$

where

$$q = \frac{K^{1-\beta}}{1-\beta}$$

and

$$u_0 = \frac{\delta q\, \gamma\rho + v_0 - v_{\min}}{\delta q\, \gamma\sqrt{1-\rho^2}}.$$

See also [9] and [12].

3.3 Simulations

In this section, we describe a simulation procedure for the SABR model with a free boundary. Suppose that we have simulated the stochastic volatility for all timesteps and paths v_t. (This is trivial for the lognormal process.) Suppose further that at timestep t and for a given path, we have simulated F_t. For the next interval $[t,\, t+\Delta t]$, we select a random normal number $Z \in N(0,1)$ and a corresponding uniform number $U = \mathcal{N}(Z)$ (ensuring proper correlation with the stochastic volatility ones). Our goal is to simulate $F_{t+\Delta t}$ given this info.

The first thing to try is an Euler scheme

$$F_{t+\Delta t} = F_t + |F_t|^\beta\, v_t\, \sqrt{\Delta t}\, Z.$$

One can explicitly check that the Euler scheme does not work for points close to zero even when $\Delta t \to 0$.

Instead of the SABR process F, we simulate the Bessel squared process X_t, given by

$$X = \text{sign}(F)\, \frac{|F|^{2(1-\beta)}}{(1-\beta)^2}$$

with the SDE

$$dX_t = 2\,\text{sign}(X_t)\,(\nu+1)\, v_t^2\, dt + 2\, v_t\, \sqrt{X_t}\, dW.$$

Setting v_t to 1 for the moment, it is easy to see that its transition density is expressed via the absorbing and reflecting solutions of the BESQ as

$$p(t,\, x,\, x_0) = \frac{1}{2}\left\{p_R(t,\, |x|,\, |x_0|) + \text{sign}(x\, x_0)\; p_A(t,\, |x|,\, |x_0|)\right\},$$

which gives the CDF $C_F(t,\, x,\, x_0) = E[1_{X_t^F < x}]$ as

$$C_F(t,\, x,\, x_0) = \frac{1}{2}\{1 + \text{sign}(x)\, E[1_{X_t^R < |x|}] - \text{sign}(x_0)\, E[1_{X_t^A > |x|}]\}.$$

In terms of the noncentral χ^2 CDF, the transition density takes the form

$$C_F(t, x, x_0) = \frac{1}{2} + \frac{1}{2}\text{sign}(x)\chi^2\left(\frac{|x|}{t}, 2\nu+2, \frac{|x_0|}{t}\right) - \text{sign}(x_0)\; \chi^2\left(\frac{|x_0|}{t}, -2\nu, \frac{|x|}{t}\right),$$

where χ^2 denotes the CDF itself. Recall that $\nu = -\frac{1}{2(1-\beta)}$ lies in the interval $(-1, 0)$ and that $(2\nu+2)$ and (-2ν) are the dimensions (both positive) of the χ^2 distribution.

We can numerically invert the free BESQ CDF to obtain the simulation scheme (restoring the stochastic volatility by $\Delta t \to \Delta t\, v_t^2$).

This is indeed very slow, and we proceed with a regime switching scheme similar to [2] in order to accelerate the simulations:

1. Calculate analytically two first moments of $X_{t+\Delta t} \mid X_t\, v_t$:

$$M_n(X_t, v_t) = \int dx\, x^n\, p(\Delta t\, v_t^2,\, x,\, X_t) \quad \text{for} \quad n = 1, 2,$$

which gives

$$M_1 = M_1^A = \left(X_t + 2(1-|\nu|)v_t^2\Delta t\right) \frac{\gamma(|\nu|, \frac{X_t}{2v_t^2\Delta t})}{\Gamma(|\nu|)} + X_t \frac{e^{-\frac{X_t}{2v_t^2\Delta t}} \left(\frac{X_t}{2v_t^2\Delta t}\right)^{|\nu|-1}}{\Gamma(|\nu|)},$$
$$M_2 = M_2^R = X_t^2 + 4(\nu+2)v_t^2\Delta t|X_t| + 4(\nu+1)(\nu+2)\left(v_t^2\Delta t\right)^2.$$

Note that it is only the absorbing part of the PDF that contributes to M_1, while only the reflecting part contributes M_2.

2. For out of boundary values, use the moment matching to approximate $X_{t+\Delta t}$ via the quadratic Gaussian step

$$X_{t+\Delta t} \sim a(1 + b\, Z)^2.$$

(The coefficients a and b are determined by the moment matching.)

3. For near-boundary values, numerically invert

$$C_F(\Delta t\, v_t^2,\, X_{t+\Delta t},\, X_t) = U.$$

We conclude with some important remarks. The simulation quality for far-from-zero points (e.g., using a simple Euler method instead of moment matching) can influence convergence but will not kill the scheme. The overall accuracy is very sensitive to the handling of the near-zero points: naive approximations can lead to wrong limits as $\Delta t \to 0$. One can treat the "absorbing" solution simulation scheme much more "roughly" than the "reflecting" and "free". For example, the "absorbing" solution can be done via a simple Euler with a floor of zero:

$$F_{t+\Delta t} = \max(F_t + |F_t|^\beta\, v_t\, \sqrt{\Delta t}\, Z, 0).$$

The time argument in the scheme $\Delta t\, v_t^2$ can eventually become large due to the stochastic vol. Thus, the SABR simulations convergence in timesteps can be much slower than that for the CEV.

4 Numerical experiments

We analyze the *normal implied volatility* (bps) for European call options $\mathcal{C}(T,K) = E[(F_T - K)^+]$ for the free-boundary SABR with the parameters that are shown in Table 4.

Parameter	Symbol	Value for Input I	Value for Input II
Rate Initial Value	F_0	50 bps	1%
SV Initial Value	v_0	$0.6\,F_0^{1-\beta}$	$0.3\,F_0^{1-\beta}$
Vol-of-Vol	γ	0.3	0.3
Correlations	ρ	-0.3	-0.3
Skews	β	0.25	0.25
Maturities	T	3Y	10Y

Table 4: Setups for the free-boundary SABR model.

In Table 5, we compare the Monte Carlo simulations (Exact) described above and our analytical formula based on the map to the zero correlation SABR model (Analyt).

	Input I			Input II		
K	**Analyt**	**Exact**	**Diff**	**Analyt**	**Exact**	**Diff**
-0.95	30.87	30.93	-0.06	40.05	40.86	-0.81
-0.8	29.83	29.95	-0.12	38.43	39.24	-0.81
-0.65	28.80	28.97	-0.17	36.80	37.60	-0.80
-0.5	27.79	27.99	-0.20	35.18	35.97	-0.78
-0.35	26.83	27.04	-0.21	33.59	34.33	-0.74
-0.2	25.95	26.15	-0.20	32.05	32.73	-0.68
-0.05	25.30	25.46	-0.16	30.67	31.25	-0.58
0.1	25.77	25.85	-0.08	30.20	30.63	-0.43
0.25	26.63	26.69	-0.06	30.19	30.51	-0.31
0.4	27.33	27.39	-0.06	30.14	30.41	-0.27
0.55	27.90	27.97	-0.06	30.06	30.31	-0.25
0.7	28.38	28.45	-0.07	30.00	30.22	-0.23
0.85	28.80	28.87	-0.07	29.98	30.18	-0.20
1	**29.18**	**29.25**	**-0.07**	**30.05**	**30.22**	**-0.17**
1.15	29.53	29.60	-0.07	30.24	30.36	-0.12
1.3	29.87	29.94	-0.07	30.56	30.63	-0.07
1.45	30.22	30.29	-0.06	31.03	31.04	-0.01
1.6	30.58	30.63	-0.06	31.63	31.58	0.04
1.75	30.95	30.99	-0.05	32.35	32.26	0.09
1.9	31.33	31.37	-0.04	33.17	33.04	0.13

Table 5: Differences in implied volatilities (in bps) for the SABR model between a Monte Carlo simulation (Exact) and our method (Analyt), where the model parameters are given in Table 4. The bold line ($K = 1$) represents the ATM strike.

The implied volatility results that are shown in Table 5 are plotted in Figure 7 (Input I) and Figure 8 (Input II).

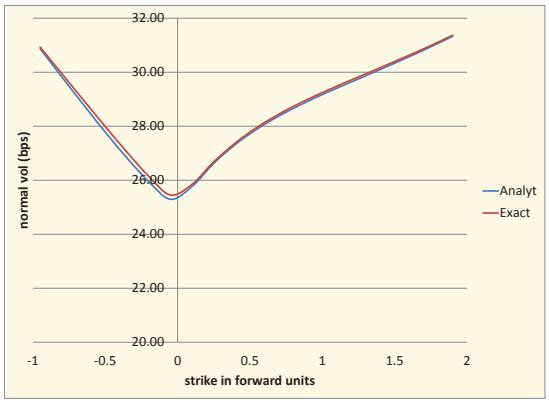

Figure 7: Plot of implied volatility for Monte Carlo simulation (Exact) and our method (Analyt) with the Input I parameters.

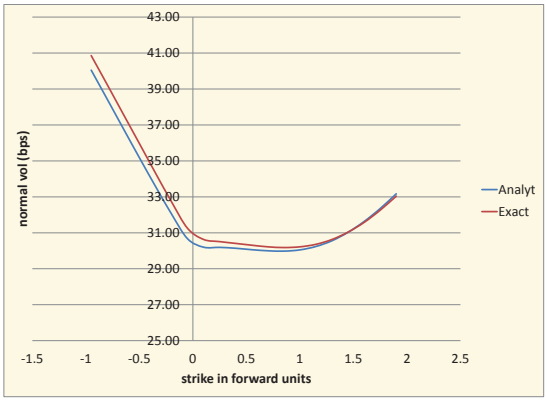

Figure 8: Plot of implied volatility for Monte Carlo simulation (Exact) and our method (Analyt) with the Input II parameters.

We observe and excellent approximation quality for 3Y and positive strikes $K > \frac{1}{2}F_0$ for 10Y and a light degeneration for other strikes. We see that the normal implied volatility possesses significant smiles with the bottom between zero and the ATM strike. In general, increasing the volatility-of-volatility and maturity moves the vertex of the smile to the ATM strike.

5 Conclusion

We have presented a natural generalization of the SABR model to negative rates, which very important in our current low-rate environment, and described its properties. We derived an exact formula for the option price in the zero-correlation case and an efficient approximation for general correlation. The simplicity of the approximation permits a straightforward implementation. Moreover, the main formulae from our "absorbing" (standard) SABR approximation can be directly reused. We have studied different MC schemes and came up with an efficient one. Finally, we have numerically checked the approximation accuracy for option pricing.

The authors are indebted to Serguei Mechkov for discussions and numerical implementation help as well as to their colleagues at Numerix, especially to Gregory Whitten and Serguei Issakov for supporting this work and Nic Trainor for the excellent editing.

References

[1] Andreasen J. and Huge B. (2013) "Expanded Forward Volatility", RISK magazine, January

[2] Andersen L. (2007) "Efficient Simulation of the Heston Stochastic Volatility Model", SSRN paper

[3] Antonov A., Konikov M. and Spector M. (2013) "SABR spreads its wings", RISK magazine, August

[4] Antonov A., Konikov M., Rufino D. and Spector M. (2014) "Exact Solution to CEV Model with Uncorrelated Stochastic Volatility", SSRN paper

[5] Balland P. and Tran Q. (2013) "SABR goes normal", Risk magazine, May

[6] Jeanblanc M., Yor M., and Chesney M. (2009) "Mathematical Methods for Financial Markets" Springer.

[7] Hagan P., Kumar D., Lesnievski A., and Woodward D., (2002) "Managing Smile Risk", Wilmott Magazine, September

[8] Hagan P., Kumar D., Lesnievski A., and Woodward D., (2014) "Arbitrage Free SABR", Wilmott Magazine, January

[9] Henry-Labordere P., "Analysis, Geometry, and Modeling in Finance: Advanced Methods in Option Pricing", Chapman & Hall (2008).

[10] Islah O.(2009), "Solving SABR in exact form and unifying it with LIBOR market model", SSRN paper

[11] Mercurio F. and Morini M. (2009) "Joining the SABR and Libor models together, Risk March, 80-85.

[12] Paulot L.(2009) "Asymptotic Implied Volatility at the Second Order with Application to the SABR Model", SSRN paper

[13] Rebonato R., McKay K. and White R. (2009) "The SABR/LIBOR Market Model: Pricing, Calibration and Hedging for Complex Interest-Rate Derivatives", John Wiley & Sons Ltd